THE JOURNAL OF PHYSICAL CHEMISTRY B

Article

pubs.acs.org/JPCB

Fluorescence Response of Coumarin-153 in *N*-Alkyl-*N*-methylmorpholinium Ionic Liquids: Are These Media More Structured than the Imidazolium Ionic Liquids?

Dinesh Chandra Khara and Anunay Samanta*

School of Chemistry, University of Hyderabad, Hyderabad-500 046, India

Supporting Information

ABSTRACT: The fluorescence behavior of coumarin-153 (C153) has been studied in four *N*-alkyl-*N*-methylmorpholinium ionic liquids differing in the alkyl chain length attached to the *N*-methylmorpholinium cation as a function of the excitation wavelength and temperature to understand some of the physicochemical characteristics of these largely unexplored ionic liquids. While the polarity of the ionic liquid with the smallest alkyl chain length is found comparable to that of the commonly used imidazolium ionic liquids, the probe molecule experiences a less polar environment with increasing chain length of the alkyl group attached to the morpholinium cation. The room temperature steady-state fluorescence spectrum of C153 in these solvents is found to be dependent on the excitation wavelength, and this effect is most pronounced in long chain containing ionic liquids. A bathochromic shift of the fluorescence maximum is observed at higher temperature. The excitation wavelength and temperature dependence of the fluorescence of C153 is explained considering a domain structure of these ionic liquids. The time-resolved fluorescence anisotropy measurements indicate the microviscosity around the probe molecule to be significantly different from the bulk viscosity of the long-chain ionic liquids. The solvent reorganization dynamics, as studied by monitoring the time-dependent fluorescence Stokes shift of C153 in these ionic liquids, is found to be slow and similar to that in imidazolium ionic liquids. The time-resolved measurements under isoviscous conditions seem to provide additional support to the organized domain structure of these ionic liquids.

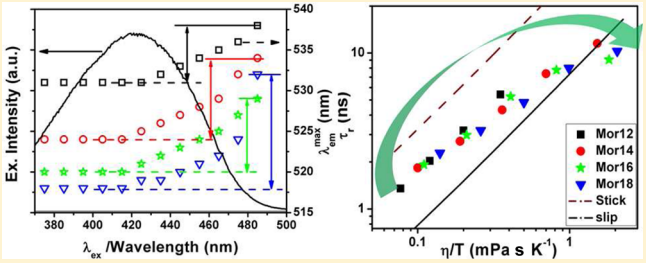

1. INTRODUCTION

The room temperature ionic liquids (ILs) continue to attract a great deal of attention primarily because of the fact that only a very few of the large number of possible ILs have so far been studied.[1−7] An additional factor contributing to the vigorous activities with these substances is the complex nature of these substances and the findings that the physicochemical properties of even some of the extensively studied ILs such as those based on imidazolium, ammonium, phosphonium, pyridinium, and pyrolidinium cations are not fully understood.[8−12] It is thus evident that the intensity with which the ILs are being studied currently from different directions will last for quite some time. ILs based on the *N*,*N*′-dialkylimidazolium salts have thus far been the most widely studied because of their favorable physical properties. However, considering the high cost of industrial scale synthesis of these salts, the focus seems to be shifting gradually toward other less expensive alternatives such as the morpholinium ILs, which are not only cheap and easy to develop but also possess good physicochemical characteristics.[13−17]

In this work, we attempt to explore some of the physicochemical properties of largely unexplored four different *N*-alkyl-*N*-methylmorpholinium ILs, abbreviated as [$Mor_{1,2}$][Tf_2N], [$Mor_{1,4}$][Tf_2N], [$Mor_{1,6}$][Tf_2N], and [$Mor_{1,8}$][Tf_2N] (Chart 1), consisting of *N*-alkyl-*N*-methylmorpholinium cation with four different alkyl chain lengths and an identical anionic component, [Tf_2N]$^-$, by probing the steady-state and time-resolved fluorescence behavior of a dipolar solute, C153, whose fluorescence properties in conventional solvents and several ILs are very well understood.[18−20] The physicochemical properties of an IL strongly depend on the constituent ions. A gradual variation of the length of the alkyl chain attached to one of the

Chart 1. Chemical Formula and Abbreviations of the ILs and Probe Molecule

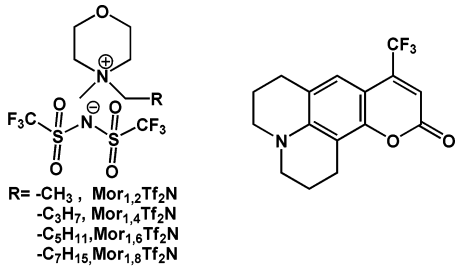

Received: June 2, 2012
Revised: October 19, 2012
Published: October 19, 2012

   dx.doi.org/10.1021/jp3054058 | *J. Phys. Chem. B* 2012, 116, 13430−13438

constituent ions is expected to vary systematically the properties of the ILs that we attempt to capture in this work. While the room temperature measurements reveal the influence of viscosity of these ILs on the fluorescence response of C153, the experiments performed under isoviscous conditions, maintained by heating the ILs to different temperatures, help in identifying the factor(s), if any, other than the viscosity of the medium that may influence the fluorescence behavior of the probe molecule. In addition to probing the steady-state fluorescence response of C153 in these ILs, we study its time-resolved behavior, from which we extract information on the dynamics of solvent reorganization and solute rotational diffusion, which is crucial to the understanding of the physicochemical characteristics of the media and their utilization.[21,22] As solvation leads to considerable Stokes shift of the fluorescence spectrum of a dipolar molecule in a polar medium, the solvation dynamics is most commonly studied by measuring the time-dependent Stokes shift of the fluorescence maximum of a dipolar probe molecule following its electronic excitation using a short pulse of light.[23,24] A large number of experimental and theoretical studies on solvation dynamics in various ILs highlight both the importance of the process and its complex nature.[11,12,20,25−49] The rotational diffusion of a solute molecule, which is commonly investigated by studying the time-resolved fluorescence anisotropy of a probe molecule, is also known to provide important information on the nature of solute−solvent interaction in these media. Hence, several studies dealing with the rotational motion of solutes in ILs have been made in recent years employing a variety of probe molecules and ILs.[29−31,34,38,39,50−56]

Several experimental and theoretical studies in recent years have indicated that most of the *N*-alkyl-*N*-methylimidazolium ILs are not homogeneous structureless liquids but possess an organized domain-like structure formed by the segregation of the alkyl chains on one hand and the charged components on the other.[57−64] An important aspect of this work, which we investigate, is the structural heterogeneity of these ILs. As the long alkyl chains are known to contribute to the heterogeneity of the ILs, we have chosen four different alkyl chains to understand the heterogeneity of the *N*-alkyl-*N*-methylmorpholinium ILs.

2. EXPERIMENTAL SECTION

2.1. Materials. C153 (laser grade, Eastman Kodak) was used as received. Alkyl bromides, acetone, acetonitrile, and dichloromethane (DCM) were obtained from Merck (India) and were distilled prior to use. *N*-Methylmorpholine and bis(trifluoromethanesulfonyl)imide lithium salt ($LiTf_2N$) were procured from Sigma Aldrich and used as received.

2.2. Synthesis of $[Mor_{1,n}][Tf_2N]$. These ILs were synthesized by following a two-step procedure.[13,14] In the first step, alkyl bromides were slowly added to the *N*-methylmorpholine solution in acetonitrile. Then, the solution was refluxed at 80 °C for 6−8 h. Subsequently, acetonitrile was removed from the reaction mixture in a rotary evaporator and the bromide salts, $[Mor_{1,n}][Br]$, were washed with acetone several times to remove the unreacted materials from the reaction mixture. Finally, the white bromide salts were dried for several hours under high vacuum. The second step involved a metathesis reaction for which $[Mor_{1,n}][Br]$ and lithium bis(trifluoromethanesulfonyl)imide were taken in DCM and stirred for 24 h. Then, the DCM solution was washed with water several times until it was free from any halide (checked with a $AgNO_3$ solution). Finally, DCM was removed from the mixture and the ILs were dried for several hours under high vacuum prior to use.

2.3. Instrumentation. The viscosities of the solvents were measured by a LVDV-III Ultra Brookfield Cone and Plate viscometer (1% accuracy and 0.2% repeatability). The viscosities at different temperatures were measured by using a water circulator (Julabo). In order to perform experiments under isoviscous conditions (η = 130 cP), the ILs, $[Mor_{1,2}Tf_2N]$, $[Mor_{1,4}][Tf_2N]$, $[Mor_{1,6}][Tf_2N]$, and $[Mor_{1,8}][Tf_2N]$, were heated at 32, 43, 45, and 47 °C, respectively. The absorption and steady-state fluorescence spectra were recorded on a UV−visible spectrophotometer (Cary100, Varian) and spectrofluorometer (FluoroLog, Horiba Jobin Yvon), respectively. The fluorescence spectra were corrected for the instrumental response. Time-resolved fluorescence and anisotropy decay measurements were carried out using a time-correlated single-photon counting (TCSPC) spectrometer (Horiba Jobin Yvon IBH). A diode laser (λ_{exc} = 405 nm) was used as the excitation source, and an MCP photomultiplier (Hamamatsu R3809U-50) was used as the detector (response time 40 ps). The instrument response function (IRF) of the setup (50 ps) was limited by the full width at half-maximum (fwhm) of the exciting laser pulse. The lamp profile was recorded by placing a scatterer (dilute solution of Ludox in water) in place of the sample. Decay curves were analyzed by a nonlinear least-squares iteration procedure using IBH DAS6 (Version 2.2) decay analysis software. The quality of the fits was assessed by the χ^2 values and distribution of the residuals. The temperature-dependent studies were performed by using a water circulator (Julabo).

2.4. Method. The time-resolved emission decay profiles of C153 were measured at 5/10 nm interval across the entire steady-state emission spectra. The fluorescence decay profiles were recorded by placing the emission polarizer at magic angle (54.7°). The wavelength selection was made by a monochromator with a bandpass of 2 nm. The total number of measurements was 26−28 in each case. Each decay curve was fitted to a triexponential decay function with an iterative reconvolution program (IBH). The time-resolved emission spectra (TRES) were constructed according to a procedure described earlier.[34] The TRES at various times were fitted to a log-normal function, as indicated below, to obtain the peak maxima at different times.

$$I = h \exp[-\ln 2\{\ln(1 + \alpha)/\gamma^2\}] \quad \text{for } \alpha > 1$$
$$= 0 \quad \text{for } \alpha \leq -1 \qquad (1)$$

where $\alpha = 2\gamma(\bar{\nu} - \bar{\nu}_{peak})/\Delta$, $\bar{\nu}_{peak}$ is the wavenumber corresponding to the peak, h is the peak height, Δ is the fwhm, and γ corresponds to the asymmetry of the band shape.

The anisotropy measurements were performed using two polarizers by placing one of them in the excitation beam path and the other in front of the detector. An alternate collection of the fluorescence intensity in parallel ($I_{\parallel}$) and perpendicular ($I_{\perp}$) polarization (with respect to the vertically polarized excitation laser beam) for equal intervals of time was made until the count difference between the two polarizations (at t = 0) was ∼5000. For *G*-factor calculation, the same procedure was followed but with only four cycles and horizontal polarization of the exciting laser beam. The anisotropy measurements were performed at the respective fluorescence maxima of the probe using a monochromator with a bandpass of 2 nm. Time-resolved

fluorescence anisotropy, $r(t)$, is calculated using the following equation

$$r(t) = \frac{I_{II}(t) - GI_{\perp}(t)}{I_{II}(t) + 2GI_{\perp}(t)} \quad (2)$$

where G is the correction factor for the detector sensitivity to the polarization direction of the emission and $I_{\parallel}(t)$ and $I_{\perp}(t)$ are the fluorescence decays polarized parallel and perpendicular to the polarization of the excitation light, respectively. The rotational time constants were estimated by fitting the anisotropy decay profiles to a single and/or a biexponential function depending on the situation.

3. RESULTS AND DISCUSSION

3.1. Steady-State Measurement. *3.1.1. Steady-State Absorption and Emission.* The room temperature (25 °C) absorption and emission spectra of C153 in four morpholinium ILs are shown in Figure 1. Even though the absorption maximum (λ_{max}^{abs}) of C153 in these ILs appears at the same wavelength (ca. 425 nm), the emission maximum (λ_{max}^{em}) shifts toward shorter wavelength with an increase in the chain length of the cationic component of the IL. One can observe ~15 nm blue shift of λ_{max}^{em} on changing of the solvent from [$Mor_{1,2}$][Tf_2N] to [$Mor_{1,8}$][Tf_2N]. The shift of λ_{max}^{em} is most prominent when the solvent is changed from [$Mor_{1,2}$][Tf_2N] to [$Mor_{1,4}$][Tf_2N]. However, on changing the solvent from [$Mor_{1,4}$][Tf_2N] to [$Mor_{1,8}$][Tf_2N], a small shift of λ_{max}^{em} is observed.

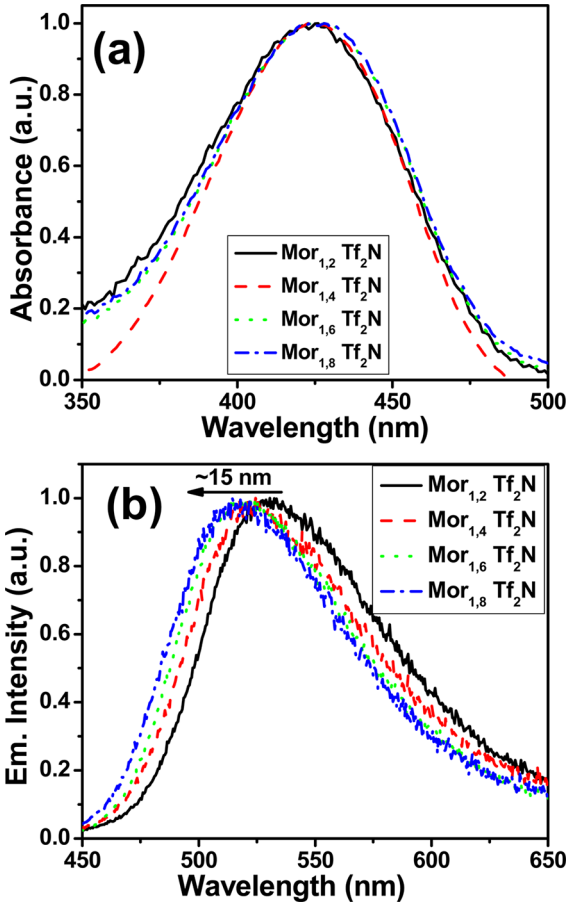

Figure 1. Normalized absorption (a) and fluorescence (b) spectra of C153 in four different morpholinium ILs at 25 °C. λ_{exc} for the emission measurements is 405 nm.

The fact that λ_{max}^{abs} of C153 appears at the same wavelength in four different ILs but λ_{max}^{em} is sensitive to the variation of the alkyl chain length of the cation is consistent with the more polar nature of the emitting state of C153 compared to the ground state.[18] It is evident from the λ_{max}^{em} values that C153 experiences a less polar environment in ILs comprising a higher alkyl chain length. This is perhaps a reflection of the fact that a longer alkyl chain length of one of the constituent ions implies a larger volume of the nonpolar region.

As C153 is a polarity sensitive probe, one can attempt to estimate the microscopic polarity experienced by the probe in these ILs from its fluorescence energy ($\bar{\nu}_{max}^{em}$) in these media. By measuring the $\bar{\nu}_{max}^{em}$ values of C153 in several conventional solvents of known polarity ($E_T(30)$) and then using the linear correlation between $\bar{\nu}_{max}^{em}$ and $E_T(30)$ and the measured $\bar{\nu}_{max}^{em}$ values in ILs, one obtains $E_T(30)$ values (Table 1) of 45.1, 45.8, 47.0, and 48.5 for [$Mor_{1,8}$][Tf_2N], [$Mor_{1,6}$][Tf_2N], [$Mor_{1,4}$]-[Tf_2N], and [$Mor_{1,2}$][Tf_2N], respectively. It thus appears that the polarity of the long chain containing ILs, [$Mor_{1,6}$][Tf_2N] and [$Mor_{1,8}$][Tf_2N], is comparable to that of acetonitrile [$E_T(30)$ = 45.6], whereas the polarity of the two short chain containing ILs, [$Mor_{1,2}$][Tf_2N] and [$Mor_{1,4}$][Tf_2N], is similar to that of long chain alcohols such as 1-octanol [$E_T(30)$ = 48.1] and cyclopentanol [$E_T(30)$ = 47], respectively.[65] These values are slightly lower than those for the corresponding imidazolium salts.[11,66] However, we show that these values do not correctly represent the true polarity of these ILs in the following section (section 3.1.2), where the basis of this statement and the correct polarity estimates of these ILs are presented.

3.1.2. Temperature Dependence of the Emission Spectra. The temperature dependence of the emission spectrum of C153 in four ILs has been studied over a range of 50 °C from 25 to 75 °C. As can be seen from Figure 2 and the data presented in Table 1, the λ_{max}^{em} values shift toward a higher wavelength with an increase in temperature. The extent of shift is dependent on the IL, and the effect is more pronounced in ILs consisting of cations with a higher chain length. For example, for a change of temperature from 25 to 55 °C, the shifts of the emission maximum observed are 105, 180, 220, and 290 cm^{-1} for [$Mor_{1,2}$][Tf_2N], [$Mor_{1,4}$][Tf_2N], [$Mor_{1,6}$]-[Tf_2N], and [$Mor_{1,8}$][Tf_2N], respectively. No further shift of the emission maximum is observed for an increase of temperature beyond 55 °C.

An increase in temperature commonly results in a blue shift of λ_{max}^{em} of dipolar molecules in conventional solvents due to a decrease of the polarity (dielectric constant) of the medium.[67] Hence, the observation of a red shift implies that the effect of a temperature induced small change in polarity of the ILs is masked by another factor, which produces a larger effect of an opposite kind. The viscosity of a medium is lowered at higher temperatures, but such change does not commonly affect the fluorescence peak position of a system in conventional solvents. However, the effect of temperature (T) on the viscosity (η) of the medium is much more pronounced in the case of ILs. The measured viscosities of the four ILs at various temperatures are shown in Figure 3 along with the curves representing the fits to the Vogel−Fulcher−Tamman equation[68]

$$\eta = \eta_0 \exp[B/(T - T_c)] \quad (3)$$

where η_0, B, and T_c are fitting parameters that depend on the IL. The high viscosity of the ILs and its strong temperature

dx.doi.org/10.1021/jp3054058 | J. Phys. Chem. B 2012, 116, 13430−13438

Table 1. Temperature Dependence of the Steady-State Fluorescence Data of the Probe Molecule (C153) and Estimated Polarity of the ILs

	$[Mor_{1,2}][Tf_2N]$		$[Mor_{1,4}][Tf_2N]$		$[Mor_{1,6}][Tf_2N]$		$[Mor_{1,8}][Tf_2N]$	
temperature (°C)	$\bar{\nu}_{em}^{max}$	$E_T(30)^a$	$\bar{\nu}_{em}^{max}$	$E_T(30)^a$	$\bar{\nu}_{em}^{max}$	$E_T(30)^a$	$\bar{\nu}_{em}^{max}$	$E_T(30)^a$
25	18830	48.5	19080	47.0	19230	45.8	19340	45.1
35	18760		18975		19160		19230	
45	18725		18900		19050		19160	
55	18725		18900		19010		19050	
65	18725		18900		19010		19050	
75	18725	49.3	18900	48.1	19010	47.3	19050	47.1

[a]Estimated from the calibration curve obtained by plotting the fluorescence maxima of C153 against known $E_T(30)$ values in conventional solvents.

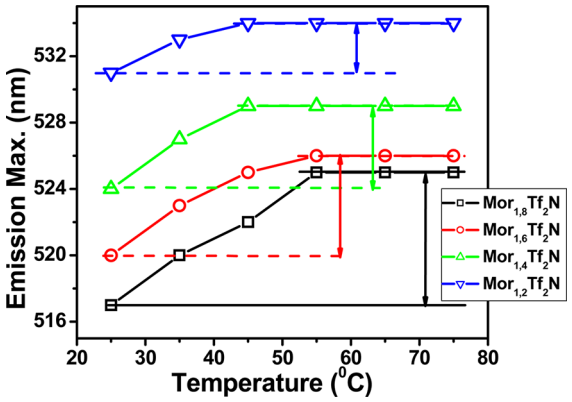

Figure 2. Temperature dependence of the fluorescence maximum (λ_{exc} = 405 nm) of C153 in the ILs.

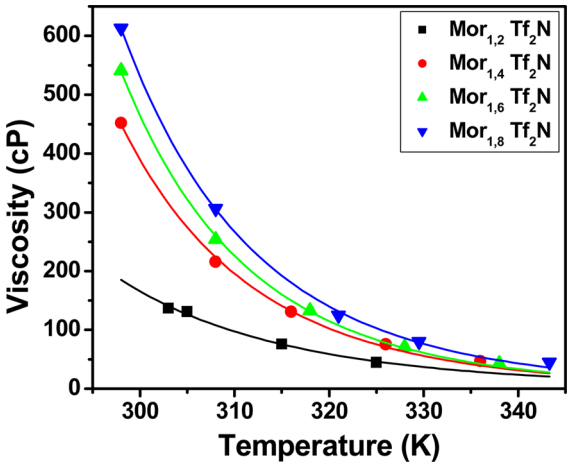

Figure 3. Measured viscosity of the morpholinium ILs at different temperatures. The solid lines represent the fits to the experimental data points according to the VFT equation.

dependence can account for the temperature dependent shift of λ_{max}^{em} of C153. It is well-known that solvent reorganization around a photoexcited dipolar molecule is a slow process in ILs due to the high viscosity of these media.[11,12,49] As a consequence, the molecules, particularly those having a fluorescence lifetime (τ_f) shorter or comparable to the solvation time ($\langle\tau_{sol}\rangle$), may not be able to emit from the completely solvated excited state at lower temperature. However, at higher temperature, due to a reduction of the viscosity of the medium, the solvation becomes faster, thereby allowing the molecules to emit from a more relaxed state. This can account for the observed temperature dependence of the λ_{max}^{em} values of C153 in the present ILs. In this context, we note that a red shift of the kind described here is reported in highly viscous (η = 800−900 cP) ammonium ILs,[39] but we are not aware of any similar report in imidazolium ILs probably because the imidazolium ILs, in which the fluorescence behavior of C153 has been studied so far, are not so viscous that the condition $\langle\tau_{sol}\rangle \geq \tau_f$ is satisfied.

The finding that even probes like C153, which has a relatively long fluorescence lifetime (τ_f = 4.8−5.2 ns), do not emit from the fully solvated state in morpholinium ILs implies that the polarities of these ILs estimated from the measured $\bar{\nu}_{max}^{em}$ values at room temperature in section 3.1.1 do not represent the correct values. However, as a constant value of $\bar{\nu}_{max}^{em}$ is reached at higher temperatures (Table 1), it can be assumed that C153 emits from the fully solvated state under these conditions and one can then use the higher temperature values of $\bar{\nu}_{max}^{em}$ for the polarity estimation. The $E_T(30)$ values estimated from the higher temperature values of $\bar{\nu}_{max}^{em}$ for $[Mor_{1,2}][Tf_2N]$, $[Mor_{1,4}][Tf_2N]$, $[Mor_{1,6}][Tf_2N]$, and $[Mor_{1,8}][Tf_2N]$, which represent the actual polarity of these media, are 49.3, 48.1, 47.3, and 47.1, respectively. As these numbers are similar to those for the imidazolium ILs with similar alkyl chain length, we conclude that the polarities of the morpholinium ILs are comparable to those of the corresponding imidazolium ILs.[11,66]

3.1.3. Excitation Wavelength Dependence of the Emission Spectra. The fluorescence behavior of C153 stated above has been measured for an excitation wavelength of 405 nm. We found that the spectral behavior remains the same as long as the excitation wavelength was $\leq\lambda_{max}^{abs}$. However, for an excitation wavelength corresponding to the tail part of the first absorption band, a red shift of the λ_{max}^{em} value is observed on increase of the excitation wavelength. This excitation wavelength dependent variation of λ_{max}^{em} is shown in Figure 4. As can be seen, the excitation wavelength dependence is most pronounced in ILs having a long alkyl chain length. It is also seen that this excitation wavelength dependence is significantly lowered with increasing temperature (Supporting Information, Figure S1).

It is documented that some dipolar molecules, when excited in their red edge of the first absorption band, display excitation wavelength dependent fluorescence spectra, which is known as the red edge effect (REE).[69] However, unlike a few other molecules, C153 does not exhibit the REE in imidazolium ILs,[11,70,71] as its fluorescence lifetime (τ_f = 5.6 ns) is considerably higher than the average solvent relaxation time ($\langle\tau_{sol}\rangle$ = 1.4−2.1 ns) of the ILs.[71] The observation of the REE of C153 in morpholinium ILs, which is more pronounced in the case of long alkyl chain containing ILs, is quite surprising, as the fluorescence lifetime of C153 in these liquids (τ_f = 4.8−5.2 ns) is still much higher than the estimated solvation time in

dx.doi.org/10.1021/jp3054058 | J. Phys. Chem. B 2012, 116, 13430−13438

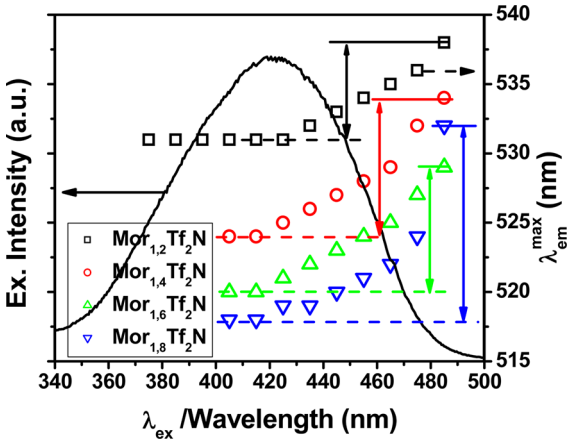

Figure 4. Excitation wavelength dependence of the emission maxima of C153 in the ILs (at 25 °C). Also shown in the figure, a typical fluorescence excitation spectrum of C153 in these ILs.

these solvents.[72] Considering this factor and noting that the REE of C153 in a highly heterogeneous medium has recently been reported,[73] we think the excitation wavelength dependent emission of C153 in these morpholinium ILs is due to the microheterogeneous nature of these media that is more prominent in the case of long chain containing ILs. It is obvious that the heterogeneity of these media arises from the segregation of the polar (the ionic constituents) and nonpolar (the alkyl chain) components of the ILs forming polar and nonpolar domains to which C153 is distributed. The lack of interaction between the molecules from different domains gives rise to emission that is dependent on the kind of molecules excited rather than that by the molecules with the lowest singlet state energy. With an increase in temperature as the domain structure is partially destroyed, the excitation wavelength dependence decreases or disappears. Therefore, the excitation wavelength dependent fluorescence behavior of C153 and its temperature dependence suggest that the morpholinium ILs are more heterogeneous than the imidazolium ILs of comparable viscosity.

A comparison of the excitation wavelength dependence data of C153 in four ILs under isoviscous conditions also presents a similar picture (Figure 5). Under this condition, one expects

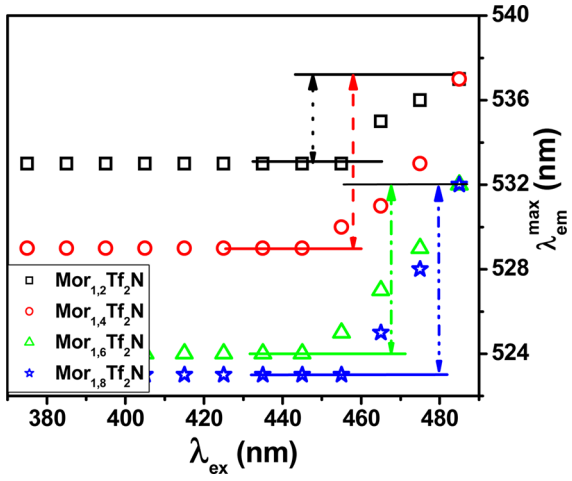

Figure 5. Excitation wavelength dependence of the emission maxima of C153 in the ILs (under isoviscous conditions, η = 130 cP).

C153 to display similar excitation wavelength dependence in all ILs. However, Figure 5 shows that this is not the case. The fact that the ILs with a longer alkyl chain length exhibit a more pronounced excitation wavelength dependence compared to the other ILs with shorter alkyl chain length under isoviscous conditions can be explained only in terms of domain-like structures for the ILs.

3.2. Time-Resolved Measurement. *3.2.1. Rotational Dynamics.* The time-resolved fluorescence measurements have been performed under both isothermal and isoviscous conditions. The measurements under the isothermal conditions are performed at 40 °C instead of room temperature (25 °C), as the decay kinetics were found too slow to be estimated accurately at room temperature, particularly in the case of long chain containing ILs. The rotational diffusion of the probe molecule has been studied by following the time dependence of the fluorescence anisotropy of the system. Representative fluorescence anisotropy decays of C153 in four ILs are shown in Figure 6. Even though these profiles are better described by a

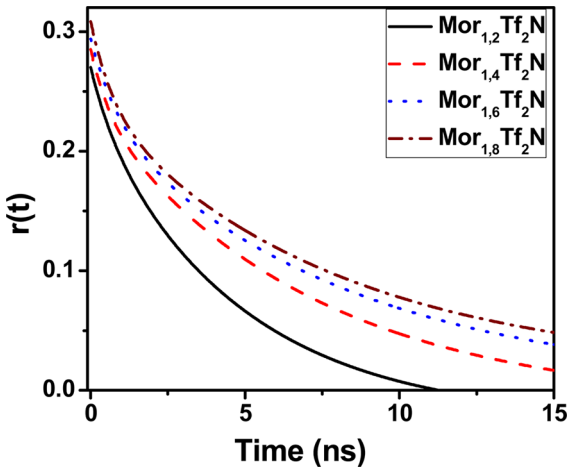

Figure 6. Anisotropy decay profiles of C153 in the ILs under isothermal conditions (40 °C). The data points are omitted for clarity.

biexponential function, the average reorientation time obtained from such analysis was found to be not very different from that obtained from the single-exponential fits to the data. The measured rotational time constants of the molecule in different ILs are collected in Table 2 together with the solvent viscosity. As can be seen, under isothermal conditions, the rotational relaxation time of C153 increases with increasing viscosity (or chain length) of the ionic liquid. However, in highly viscous $[Mor_{1,6}][Tf_2N]$ and $[Mor_{1,8}][Tf_2N]$, the rotational time constants are very similar.

According to the Stokes–Einstein–Debye (SED) hydrodynamic theory,[22,29] at any given temperature (T), the reorientation time of a solute rotating in a solvent continuum is proportional to $(1/\eta)$, where η is the viscosity of the medium. Hence, in the absence of any specific interaction between the solvent and probe molecule, the observations of a very similar reorientation time of C153 in two highly viscous ILs, $[Mor_{1,6}][Tf_2N]$ and $[Mor_{1,8}][Tf_2N]$, whose bulk viscosities differ by 34 cP, and also a faster rotation of the probe in these media compared to that in two less viscous ILs, $[Mor_{1,2}][Tf_2N]$ and $[Mor_{1,4}][Tf_2N]$, are contrary to the SED hydrodynamic prediction. These results can only be understood when these ILs, in particular, those with the long chain lengths, are

dx.doi.org/10.1021/jp3054058 | J. Phys. Chem. B 2012, 116, 13430–13438

Table 2. Rotational Relaxation Time of C153 in Different ILs under Isothermal (40 °C) and Isoviscous (η = 130 cP) Conditions

ILs	viscosity[a] (cP)	$\langle\tau_{rot}\rangle^b$ (T = 40 °C)	$C_{rot}{}^c$	viscosity[d] (cP)	$\langle\tau_{rot}\rangle^b$ (isoviscous)	$C_{rot}{}^c$
$[Mor_{1,2}][Tf_2N]$	82	4.3	0.55	130	5.9	0.46
$[Mor_{1,4}][Tf_2N]$	157	5.9	0.39		5.5	0.45
$[Mor_{1,6}][Tf_2N]$	180	6.4	0.37		5.4	0.44
$[Mor_{1,8}][Tf_2N]$	214	6.2	0.30		4.7	0.39

[a]At 40 °C, estimated from the plots shown in Figure 3. [b]Average rotational time (ns), $\langle\tau_{rot}\rangle = a_1\tau_{r1} + a_2\tau_{r2}$, where $a_1 + a_2 = 1$, ±5%. [c]$C_{rot} = \tau_r{}^{exp}/\tau_r{}^{stick}$. [d]Experimentally measured viscosity at 32, 43, 45, and 47 °C for $[Mor_{1,2}][Tf_2N]$, $[Mor_{1,4}][Tf_2N]$, $[Mor_{1,6}][Tf_2N]$, and $[Mor_{1,8}][Tf_2N]$, respectively.

considered to be structured liquid rather than a continuum, as assumed in the SED theory. The results suggest that the microviscosity around the probe molecule is lower than the bulk viscosity of the medium.

These results can also be analyzed from another angle. As $C_{rot} = \tau_r$ (expt)/τ_r(theo), it is a measure of the association of the solute with the solvent molecules or a ratio of the actual hydrodynamic volume to the stick hydrodynamic volume. Other factors remaining the same, an increase in the size of the solvent molecule due to an increase in the alkyl chain length is expected to increase the C_{rot} value. However, this is not the case here (Table 2). The C_{rot} values indicate a lesser degree of association with an increase in the size of the solvent. This can only be explained if there occurs a phase separation into hydrophobic and hydrophilic domains with an increase in the size of the solvent and localization of the probe molecule in the nonpolar domain.

The anisotropy decay profiles were measured, and the rotational time constants are estimated (Table 2) also under isoviscous conditions (η = 130 cP) by heating the four ILs to different temperatures. As can be seen from Table 2, C153 shows a similar rotational relaxation time constant except in $[Mor_{1,8}][Tf_2N]$, where a relatively faster decay of the anisotropy is observed. The observation seems to imply that the microheterogeneous domain structure of $[Mor_{1,8}][Tf_2N]$ still persists even at a higher temperature (47 °C) and C153 is located in a region which is less viscous than the bulk viscosity of the medium (130 cP).

Apart from the studies carried out under isothermal and isoviscous conditions, we have measured the temperature dependence of the rotational relaxation time constant over a wide range of temperature (25−65 °C) in these ionic liquids. The results are depicted in Figure 7. The plot of τ_r versus η/T indicates that the τ_r values of C153 lie between the slip and stick boundary condition of the SED theory. It is interesting to note, however, the deviation from the linearity in long chain containing ionic liquids. The degree of the nonlinearity in each set is evident from the fitting parameters, when the data is fit to $\tau_r = A(\eta/T)^p$.

C153 in $[Mor_{1,2}][Tf_2N]$

$$\tau_r = (14.25 \pm 0.25)\left(\frac{\eta}{T}\right)^{0.92\pm0.012} \qquad (N = 4,\ R = 0.9997)$$

C153 in $[Mor_{1,4}][Tf_2N]$

$$\tau_r = (8.80 \pm 0.17)\left(\frac{\eta}{T}\right)^{0.67\pm0.03} \qquad (N = 5,\ R = 0.9959)$$

C153 in $[Mor_{1,6}][Tf_2N]$

$$\tau_r = (7.31 \pm 0.50)\left(\frac{\eta}{T}\right)^{0.48\pm0.08} \qquad (N = 5,\ R = 0.9311)$$

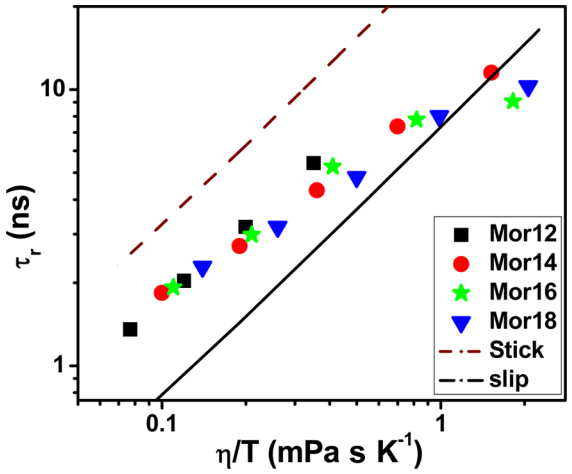

Figure 7. Plot of rotational time constant (τ_r) versus η/T in different ionic liquids. The slip (solid) and stick (dash) lines are computed by using V = 246 Å^3, f = 1.71, and C = 0.24 (taken from ref 35).

C153 in $[Mor_{1,8}][Tf_2N]$

$$\tau_r = (7.20 \pm 0.30)\left(\frac{\eta}{T}\right)^{0.54\pm0.05} \qquad (N = 5,\ R = 0.9777)$$

Except for $[Mor_{1,2}][Tf_2N]$, the p values for these ionic liquids lie between 0.48 and 0.67. This is in contrast to the findings of most of the rotational dynamics studies in ionic liquids, which report p values close to 1.[50−55] It is also known that the "p" values are close to 1 for all common organic solvents except for higher n-alkanes, where this value is around 0.63.[74,75] The deviation in the plot of τ_r versus η/T from the slip boundary condition at low temperature and a decrease in the coupling constant ($C_{rot} = \tau_r/\tau_{stick}$) for long chain containing ionic liquids is similar to the rotational behavior of C153 in higher n-alkanes,[74] which was attributed to inefficient solvent packing around the rotating solute. In another study, a very similar rotational behavior of C153 in molten salt is explained in terms of the domain structure of the medium at low temperature.[75] Considering this literature, we explain our results in terms of the heterogeneity of the ionic liquids, where a domain structure is formed by the alkyl group of the ionic liquids in one hand and charged constituents of the ionic liquids on the other.[57−64] It appears that with an increase in the chain length of the ionic liquids the probe molecule prefers to reside in the nonpolar domain, formed by the alkyl group and this is why a deviation from the SED model, similar to that observed in higher n-alkanes, is observed in long chain containing ionic liquids.

Though excitation wavelength dependent study is another approach for probing the heterogeneity of the medium,[35] in the present case, an excitation wavelength dependent study (λ_{exc} = 375, 405, and 439 nm) did not show any significant variation of the rotational time constant. However, from this observation,

dx.doi.org/10.1021/jp3054058 | J. Phys. Chem. B 2012, 116, 13430−13438

we cannot comment on the presence/absence of the heterogeneity of these ionic liquids mainly because we could not excite at the red-edge of the absorption band of the molecule with these wavelengths. One needs to use longer wavelength excitation and carry out experiments with additional probe molecules to arrive at a definite conclusion.

3.2.2. Solvation Dynamics. The time-resolved emission spectra of C153, constructed from the wavelength dependent fluorescence decay profiles according to the procedure described in the Experimental Section, show a time-dependent shift of the emission maximum from higher energy to lower energy (Figure 8), indicating slow solvent-mediated relaxation

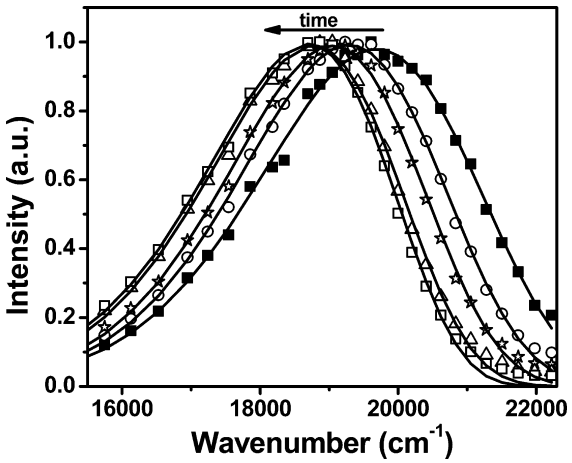

Figure 8. Normalized TRES of C153 in $[Mor_{1,2}][Tf_2N]$ (at 40 °C): (■) 0 ps, (○) 100 ps, (☆) 250 ps, (△) 1000 ps, (□) 2000 ps.

of the excited state of the probe. The total time-dependent Stokes shift estimated from the measured wavenumbers corresponding to the fluorescence maxima at zero and infinite times are found to be 1045, 1235, 1140, and 1360 cm^{-1} at 40 °C for $[Mor_{1,2}][Tf_2N]$ to $[Mor_{1,8}][Tf_2N]$, respectively. The ultrafast component of the dynamics, which is missed here due to the finite time resolution of our single photon counting setup, is estimated by calculating the expected time-zero spectrum using a literature procedure.[76] The missing component of the total solvent reorganization dynamics is ~40−60% and found to be dependent on the chain length of the cation (Table 3). The results suggest that, at a given temperature, the missing component of the total solvent reorganization dynamics decreases with an increase in the alkyl length of the ionic liquid.

The time constant of the observable, slow component of the solvent reorganization dynamics is estimated by measuring the peak frequencies of the spectra at various times (t = 0, t, and ∞) and then analyzing the time dependence of the spectral shift correlation function, $C(t)$, defined as

$$C(t) = [\bar{\nu}(t) - \bar{\nu}(\infty)]/[\bar{\nu}(0) - \bar{\nu}(\infty)] \quad (4)$$

The time dependent decay of $C(t)$ was found to be better described by a biexponential function of the form $C(t) = \alpha_1 \exp(-t/\tau_1) + \alpha_2 \exp(-t/\tau_2)$, where τ_1 and τ_2 are the solvent relaxation times and α_1 and α_2 are the normalized pre-exponential factors. Representative plots of the data and biexponential fits to those are shown in Figure 9. The individual

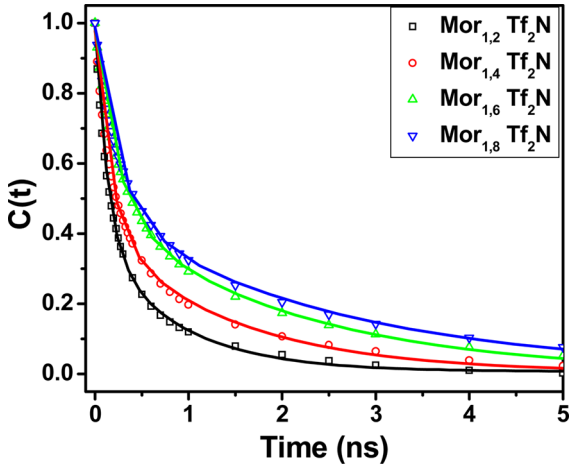

Figure 9. Decay of the spectral shift corelation function, $C(t)$, in different ILs under isothermal conditions (40 °C). Solid lines represent the biexponential fits to the data points.

fast and slow components of the dynamics along with the average values of the solvent relaxation times are collected in Table 3. It is evident that both the fast and slow components of the dynamics depend on the chain length on the cation and with increasing viscosity of the medium the dynamics becomes slow. It can also be seen (Table 3) that the average solvent relaxation time increases with the increase of the substituted alkyl chain length, i.e., viscosity of the medium. The correlation between average solvation time and the viscosity of the ILs is illustrated in Figure 10.

Under an isoviscous condition (η = 130 cP), the extent of the missing or ultrafast component of the solvent reorganization dynamics is found to be similar in all ILs; i.e., no effect of the chain length is observable on this component (Table 4). However, of the two time-resolvable components of the solvation dynamics, the shorter component does not vary significantly with the ILs, but the longer component depends on the chain length of the cation. In fact, the latter is slower by a factor of ~2 in $[Mor_{1,6}][Tf_2N]$ and $[Mor_{1,8}][Tf_2N]$ compared to $[Mor_{1,2}][Tf_2N]$ and $[Mor_{1,4}][Tf_2N]$. Consequently, despite

Table 3. Solvent Relaxation Parameters Estimated from the TRES of C153 under Isothemal Conditions (40 °C)

		relaxation data[b]					
ILs	viscosity[a] (cP)	τ_1 (a_1)	τ_2 (a_2)	$\langle\tau_{sol}\rangle$[c]	$\bar{\nu}(0)$ (cm^{-1})	observed shift ($\Delta\bar{\nu}$) (cm^{-1})	missing comp.[d]
$Mor_{1,2}Tf_2N$	82	0.14 (0.62)	0.87 (0.38)	0.41	19685	1045	60%
$Mor_{1,4}Tf_2N$	157	0.17 (0.58)	1.42 (0.42)	0.69	20015	1235	50%
$Mor_{1,6}Tf_2N$	180	0.24 (0.53)	2.05 (0.47)	1.09	20020	1140	52%
$Mor_{1,8}Tf_2N$	214	0.25 (0.53)	2.50 (0.47)	1.31	20250	1360	43%

[a]At 40 °C, estimated from the plots shown in Figure 3. [b]Using $C(t) = a_1 \exp(-t/\tau_1) + a_2 \exp(-t/\tau_2)$, where τ_1 and τ_2 are in ns. [c]Average solvation time (ns), $\langle\tau_{sol}\rangle = a_1\tau_1 + a_2\tau_2$, where $a_1 + a_2 = 1$, ±5%. The numbers in parentheses indicate the weighted amplitude. [d]Calculated according to ref 76.

dx.doi.org/10.1021/jp3054058 | J. Phys. Chem. B 2012, 116, 13430−13438

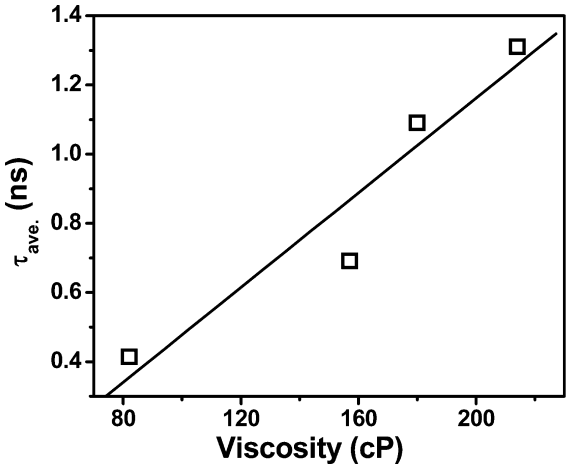

Figure 10. Viscosity dependence of the average solvation time in the ILs. The data points presented here were collected at 40 °C. The solid line represents the linear fit to the data points.

Table 4. Solvent Relaxation Parameters Estimated from the TRES of C153 under Isoviscous Conditions (η = 130 cP)

		Relaxation Data[c]			
ILs (T/°C)[a]	η[b] (cP)	τ_1 (a_1)	τ_2 (a_2)	$\langle\tau_{sol}\rangle$[d]	missing comp.[e]
$Mor_{1,2}Tf_2N$ (32)	~130	0.17 (0.64)	1.39 (0.36)	0.58	53%
$Mor_{1,4}Tf_2N$ (43)		0.15 (0.59)	1.12 (0.41)	0.55	51%
$Mor_{1,6}Tf_2N$ (45)		0.22 (0.55)	1.88 (0.45)	0.97	55%
$Mor_{1,8}Tf_2N$ (47)		0.25 (0.58)	2.04 (0.42)	1.00	49%

[a]Temperature at which the experiments were performed. [b]Experimentally measured viscosity values. [c]Using $C(t) = a_1 \exp(-t/\tau_1) + a_2 \exp(-t/\tau_2)$, where τ_1 and τ_2 are in ns. [d]Average solvation time (ns), $\tau_{av} = a_1\tau_1 + a_2\tau_2$, where $a_1 + a_2 = 1$, ±5%. The numbers in parentheses indicate the weighted amplitude. [e]Calculated according to ref 76.

having an identical viscosity, the average solvation time of C153 in long chain length containing ILs is much higher than that in short chain length containing solvents.

Maroncelli and his co-workers[35] observed that $\langle\tau_{solv}\rangle$ of a large number of ionic liquids is dependent on the size of the constituent cation (R_+) as $\langle\tau_{solv}\rangle \propto (\eta/T)^p R_+^q$ (where p = 1, q = 4, and R_+ = radius of the cation). On examination of the dependence of the average solvation time on the size of the cation according to the given equation, we found that the plot of $\langle\tau_{solv}\rangle$ versus $(\eta/T)^1 R_+^4$ gives nice correlation (R^2 = 0.958) compared to the $\langle\tau_{solv}\rangle$ versus (η/T) plot (R^2 = 0.825) under isothermal conditions. However, a plot of $\langle\tau_{solv}\rangle$ versus $(\eta/T)^1 R_+^4$ with the isoviscous condition results gives a rather poor correlation (R^2 = 0.724). Thus, it is evident that the solvation time of a probe molecule is governed not only by the bulk viscosity and size of the large ion when the organized structure of the medium comes into the picture.

4. CONCLUSION

Some of the physicochemical characteristics of four morpholinium ILs with different alkyl chain lengths attached to the cation have been probed by studying the fluorescence behavior of C153 as a function of the excitation wavelength and temperature. The excitation wavelength and temperature dependent studies seem to suggest that these *N*-alkyl-*N*-methylmorpholinium ILs are more structured and heterogeneous than the imidazolium ILs. Time-resolved fluorescence anisotropy measurements reveal that C153 is located in an environment whose viscosity is different from the bulk viscosity of the ionic liquid. While the solvation reorganization dynamics under isothermal conditions is found to be similar to that in imidazolium ILs, these measurements under isoviscous conditions suggest that the slow component of the dynamics is not necessarily dictated by the viscosity of the medium alone. Overall, a more organized domain structure of these *N*-alkyl-*N*-methylmorpholinium ILs, particularly for the long chain containing ones, is indicated in this study.

■ ASSOCIATED CONTENT

Supporting Information

Excitation wavelength dependence of the fluorescence maxima of C153 in $[Mor_{1,8}][Tf_2N]$ at different temperatures (Figure S1); anisotropy decay profiles of C153 in the ionic liquids under isoviscous conditions (η = 130 cP) (Figure S2); decay of the spectral shift corelation function, $C(t)$, in the ionic liquids under isoviscous conditions (130 cP) (Figure S3); emission contribution from neat ILs with respect to the emission from C153 (Figure S4); fitting parameters of the temperature dependence of the viscosity data according to the VFT equation (Table S1). This material is available free of charge via the Internet at http://pubs.acs.org.

■ AUTHOR INFORMATION

Corresponding Author

*E-mail: assc@uohyd.ernet.in.

Notes

The authors declare no competing financial interest.

■ ACKNOWLEDGMENTS

This work has been supported by the J.C. Bose Fellowship (to A.S.) of the Department of Science and Technology, Government of India. We thank Mr. K. Karthik for initiating some of the early experiments involving the synthesis of these ILs during his project work. D.C.K. thanks Council of Scientific and Industrial Research for a fellowship.

■ REFERENCES

(1) Hallett, J. P.; Welton, T. *Chem. Rev.* **2011**, *111*, 3508−3576.
(2) Dupont, J. *Acc. Chem. Res.* **2011**, *44*, 1223−1231.
(3) Plechkova, N. V.; Seddon, K. R. *Chem. Soc. Rev.* **2008**, *37*, 123−150.
(4) Ionic Liquids (special issue on ionic liquids). *Acc. Chem. Res.* **2007**, *40*, 1077−1236.
(5) The Physical Chemistry of Ionic Liquids (special issue on ionic liquids). *J. Phys. Chem. B* **2007**, *111*, 4639−5029.
(6) Physical Chemistry of Ionic Liquids (special issue on ionic liquids). *Phys. Chem. Chem. Phys.* **2010**, *12*, 1629−2032.
(7) Hough, W. L.; Rogers, R. D. *Bull. Chem. Soc. Jpn.* **2007**, *80*, 2262−2269.
(8) Kobrak, M. N. The Chemical Environment of Ionic Liquids: Links between Liquid Structure. In *Dynamics, and Solvation Advances in Chemical Physics*; Rice, S. A., Ed.; John Wiley & Sons, Inc.: 2008; Vol. *139*, pp 83−135.
(9) Weingärtner, H. *Angew. Chem., Int. Ed.* **2008**, *47*, 654−670.
(10) Castner, E. W., Jr.; Wishart, J. F. *J. Chem. Phys.* **2010**, *132*, 120901-1−120901-8.
(11) Samanta, A. *J. Phys. Chem. B* **2006**, *110*, 13704−13716.
(12) Samanta, A. *J. Phys. Chem. Lett.* **2010**, *1*, 1557−1562.

(13) Kim, K. S.; Choi, S.; Demberelnyamba, D.; Lee, H.; Oh, J.; Lee, B. B.; Mun, S. J. *Chem. Commun.* **2004**, 828−829.
(14) Galinski, M.; Stepniak, I. *J. Appl. Electrochem.* **2009**, *39*, 1949−1953.
(15) Lava, K.; Binnemans, K.; Cardinaels, T. *J. Phys. Chem. B* **2009**, *113*, 9506−9511.
(16) Brigouleix, C.; Anouti, M.; Jacquemin, J.; Caillon-Caravanier, M.; Galiano, H.; Lemordant, D. *J. Phys. Chem. B* **2010**, *114*, 1757−1766.
(17) Yu, W.; Peng, H.; Zhang, H.; Zhou, X. *Chin. J. Chem.* **2009**, *27*, 1471−1475.
(18) Samanta, A.; Fessenden, R. W. *J. Phys. Chem. A* **2000**, *104*, 8577−8582.
(19) Chapman, C. F.; Maroncelli, M. *J. Phys. Chem.* **1991**, *95*, 9095−9114.
(20) Karmakar, R.; Samanta, A. *J. Phys. Chem. A* **2002**, *106*, 4447−4452.
(21) Lakowicz, J. R. *Principles of Fluorescence Spectroscopy*, 3rd ed.; Springer Science: New York, 2006.
(22) Fleming, G. R. *Chemical Applications of Ultrafast Spectroscopy*; Oxford University Press: 1986.
(23) Bagchi, B.; Oxtoby, D. W.; Fleming, G. R. *Chem. Phys.* **1984**, *86*, 257−267.
(24) Maroncelli, M.; Fleming, G. R. *J. Chem. Phys.* **1987**, *86*, 6221−6239.
(25) Karmakar, R.; Samanta, A. *J. Phys. Chem. A* **2002**, *106*, 6670−6675.
(26) Karmakar, R.; Samanta, A. *J. Phys. Chem. A* **2003**, *107*, 7340−7346.
(27) Chakrabarty, D.; Harza, P.; Chakraborty, A.; Seth, D.; Sarkar, N. *Chem. Phys. Lett.* **2003**, *381*, 697−704.
(28) Arzhantsev, S.; Ito, N.; Heitz, M.; Maroncelli, M. *Chem. Phys. Lett.* **2003**, *381*, 278−286.
(29) Ingram, J. A.; Moog, R. S.; Ito, N.; Biswas, R.; Maroncelli, M. *J. Phys. Chem. B* **2003**, *107*, 5926−5932.
(30) Ito, N.; Arzhantsev, S.; Heitz, M.; Maroncelli, M. *J. Phys. Chem. B* **2004**, *108*, 5771−5777.
(31) Ito, N.; Arzhantsev, S.; Maroncelli, M. *Chem. Phys. Lett.* **2004**, *396*, 83−91.
(32) Saha, S.; Mandal, P. K.; Samanta, A. *Phys. Chem. Chem. Phys.* **2004**, *6*, 3106−3110.
(33) Mandal, P. K.; Samanta, A. *J. Phys. Chem. B* **2005**, *109*, 15172−15177.
(34) Paul, A.; Samanta, A. *J. Phys. Chem. B* **2007**, *111*, 4724−4731.
(35) Jin, H.; Baker, G. A.; Arzhantsev, S.; Dong, J.; Maroncelli, M. *J. Phys. Chem. B* **2007**, *111*, 7291−7302.
(36) Chowdhury, P. K.; Halder, M.; Sanders, L.; Calhoun, T.; Anderson, J. L.; Armstrong, D. W.; Song, X.; Petrich, J. W. *J. Phys. Chem. B* **2004**, *108*, 10245−10255.
(37) Mukherjee, P.; Crank, J. A.; Sharma, P. S.; Wijeratne, A. B.; Adhikary, R.; Bose, S.; Armstrong, D. W.; Petrich, J. W. *J. Phys. Chem. B* **2008**, *112*, 3390−3396.
(38) Adhikari, A.; Sahu, K.; Dey, S.; Ghosh, S.; Mandal, U.; Bhattacharyya, K. *J. Phys. Chem. B* **2007**, *111*, 12809−12816.
(39) Funston, A. M.; Fadeeva, T. A.; Wishart, J. F.; Castner, E. W., Jr. *J. Phys. Chem. B* **2007**, *111*, 4963−4977.
(40) Khara, D. C.; Samanta, A. *Indian J. Chem.* **2010**, *49A*, 714−720.
(41) Shim, Y.; Kim, H. J. *J. Phys. Chem. B* **2008**, *112*, 11028−11038.
(42) Kobrak, M. N.; Znamenskiy, V. *Chem. Phys. Lett.* **2004**, *395*, 127−132.
(43) Halder, M.; Headley, L. S.; Mukherjee, P.; Song, X.; Petrich, J. W. *J. Phys. Chem. A* **2006**, *110*, 8623−8626.
(44) Kashyap, H. K.; Biswas, R. *J. Phys. Chem. B* **2008**, *112*, 12431−12438.
(45) Kashyap, H. K.; Biswas, R. *J. Phys. Chem. B* **2010**, *114*, 254−268.
(46) Kashyap, H. K.; Biswas, R. *Indian J. Chem., Sect. A* **2010**, *49*, 685−694.
(47) Muramatsu, M.; Nagasawa, Y.; Miyasaka, H. *J. Phys. Chem. A* **2011**, *115*, 3886−3894.
(48) Fukazawa, H.; Ishida, T.; Shirota, H. *J. Phys. Chem. B* **2011**, *115*, 4621−4631.
(49) Maroncelli, M.; Zhang, X. X.; Liang, M.; Roy, D.; Ernsting, N. P. *Faraday Discuss.* **2012**, *154*, 409−424.
(50) Khara, D. C.; Samanta, A. *Phys. Chem. Chem. Phys.* **2010**, *12*, 7671−7677.
(51) Dutt, G. B. *J. Phys. Chem. B* **2010**, *114*, 8971−8977.
(52) Dutt, G. B. *Indian J. Chem., Sect. A* **2010**, *49*, 127−132.
(53) Karve, L.; Dutt, G. B. *J. Phys. Chem. B* **2011**, *115*, 725−729.
(54) Karve, L.; Dutt, G. B. *J. Phys. Chem. B* **2012**, *116*, 1824−1830.
(55) Fruchey, K.; Fayer, M. D. *J. Phys. Chem. B* **2010**, *114*, 2840−2845.
(56) Das, S. K.; Sarkar, M. *J. Phys. Chem. B* **2012**, *116*, 194−202.
(57) Lopes, J.; Padua, A. A. H. *J. Phys. Chem. B* **2006**, *110*, 3330−3335.
(58) Wang, Y. T.; Voth, G. A. *J. Phys. Chem. B* **2006**, *110*, 18601−18608.
(59) Xiao, D.; Rajian, J. R.; Li, S. F.; Bartsch, R. A.; Quitevis, E. L. *J. Phys. Chem. B* **2006**, *110*, 16174−16178.
(60) Triolo, A.; Russina, O.; Bleif, H. J.; Di Cola, E. *J. Phys. Chem. B* **2007**, *111*, 4641−4644.
(61) Iwata, K.; Okajima, H.; Saha, S.; Hamaguchi, H. *Acc. Chem. Res.* **2007**, *40*, 1174−1181.
(62) Yamaguchi, T.; Miyake, S.; Koda, S. *J. Phys. Chem. B* **2010**, *114*, 8126−8133.
(63) Annapureddy, H. V. R.; Kashyap, H. K.; Biase, P. M. D.; Margulis, C. J. *J. Phys. Chem. B* **2010**, *114*, 16838−16846.
(64) Russina, O.; Triolo, A.; Gontrani, L.; Caminiti, R. *J. Phys. Chem. Lett.* **2012**, *3*, 27−33.
(65) Reichardt, C. *Solvents and Solvent Effects in Organic Chemistry*, 2nd ed.; VCH Verlagsgesellschaft: 1988.
(66) Reichardt, C. *Green Chem.* **2005**, *7*, 339−351.
(67) Dobek, K. *J. Fluoresc.* **2011**, *21*, 1547−1557.
(68) Santhosh, K.; Banerjee, S.; Rangaraj, N.; Samanta, A. *J. Phys. Chem. B* **2010**, *114*, 1967−1974.
(69) Demchenko, A. P. *Luminescence* **2002**, *17*, 19−42.
(70) Mandal, P. K.; Paul, A.; Samanta, A. *J. Photochem. Photobiol., A* **2006**, *182*, 113−120.
(71) Mandal, P. K.; Sarkar, M.; Samanta, A. *J. Phys. Chem. A* **2004**, *108*, 9048−9053.
(72) As the $\langle\tau_{sol}\rangle$ values of C153 in morpholinium ILs (0.41−1.31 ns, Table 3) are estimated at 40 °C, whereas the excitation wavelength dependence (Figure 4) is studied at 25 °C, it is necessary to make necessary correction of the solvation time from its temperature dependence before comparison. Using the viscosity dependence of $\langle\tau_{sol}\rangle$ (Figure 10) and known viscosity of these ILs at 25 °C, one can obtain the $\langle\tau_{sol}\rangle$ values at 25 °C. These values range between 2.8 and 3.9 ns, which are still significantly lower than the long fluorescence lifetime (τ_f = 4.8−5.2 ns) of C153.
(73) Ghatak, C.; Rao, V. G.; Ghosh, S.; Mandal, S.; Sarkar, N. *J. Phys. Chem. B* **2011**, *115*, 12514−12520.
(74) Horng, M.-L.; Gardecki, J. A.; Maroncelli, M. *J. Phys. Chem. A* **1997**, *101*, 1030−1047.
(75) Guchhait, B.; Gazi, H. A. R.; Kashyap, H. K.; Biswas, R. *J. Phys. Chem. B* **2010**, *114*, 5066−5081.
(76) Fee, R. S.; Maroncelli, M. *Chem. Phys.* **1994**, *183*, 235−247.